MESHLESS DETECTION OF AN INTERNAL MOVING BOUNDARY

M.C. DAWSON[1], D.J. BORMAN[1], R.B. HAMMOND[1], D. LESNIC[2] and D. RHODES[3]

[1]*School of Process, Environment and Materials Engineering, University of Leeds, Leeds LS2 9JT, UK*
[2]*Department of Applied Mathematics, University of Leeds, Leeds LS2 9JT, UK*
[3]*National Nuclear Laboratory, Sellafield, Seascale, Cumbria CA20 1PG, UK*
E-mail: pm09mcd@leeds.ac.uk

Abstract. In this paper, we develop the meshless method of fundamental solutions (MFS) for solving the two-dimensional time-dependent heat equation, to locate an internal moving boundary. The inverse problem presented here is ill-posed and nonlinear and therefore, a least-squares minimisation routine is employed to reconstruct the inclusion, using known Dirichlet and Neumann boundary data on the outer fixed boundary.

1. INTRODUCTION

This article employs a thermographic method to deduce internal defects within a bounded planar domain by numerically solving the two-dimensional time dependent heat equation. This inverse method allows an internal image of the domain to be reconstructed, non-intrusively, enabling both freely moving and stationary boundaries within the domain to be tracked throughout time. The principle of tracking internal boundaries is of great importance within a vast range of engineering disciplines and also within a medical environment. Applications such as cavity and inclusion detection, and non invasive body scanning could make great use of this technique. Similar techniques have been used with other equations, such as the Laplace and Helmholtz equations, to solve steady-state geometric inverse problems of a similar nature [1,3,4]. Another area of problems, less common when solving inverse problems, however applicable when finding moving boundaries, are Stefan type problems. Stefan problems are a particular type of initial boundary value problems which contain an internal moving boundary, e.g. the melting of ice in water. Most work when solving heat related inverse problems using the MFS, has been restricted to either time-dependent one-dimensional problems or problems not depending on time, hence work discussed here has much potential when considering real world problems.

In this paper we develop the MFS for solving the two-dimensional transient heat equation which tracks a non-stationary internal boundary. The specific purpose of this moving boundary problem will be to investigate in the future the phase change scenario of a precipitation/dissolution reaction in applications containing potentially hazardous substances.

2. MATHEMATICAL FORMULATION

The mathematical formulation of the inverse geometric problem under investigation requires finding the temperature u and the moving internal defect $D(t)$ satisfying the heat equation,

$$\frac{\partial u}{\partial t}(\mathbf{x}, t) - \Delta u(\mathbf{x}, t) = 0, \quad (\mathbf{x}, t) \in (\Omega \setminus \overline{D(t)}) \times (0, T], \tag{1}$$

subject to the initial condition,

$$u(\mathbf{x}, 0) = u_0(\mathbf{x}), \quad \mathbf{x} \in \overline{\Omega} \setminus D(0), \tag{2}$$

the Cauchy (Dirichlet + Neumann) boundary conditions on the fixed outer boundary $\partial \Omega$,

$$u(\mathbf{x}, t) = f(\mathbf{x}, t), \quad (\mathbf{x}, t) \in \partial \Omega \times [0, T], \tag{3}$$

$$\frac{\partial u}{\partial n}(\mathbf{x}, t) = g(\mathbf{x}, t), \quad (\mathbf{x}, t) \in \partial\Omega \times [0, T], \tag{4}$$

and the Dirichlet or Neumann boundary condition on $\partial D(t)$, namely,

$$u(\mathbf{x}, t) = h(\mathbf{x}, t), \quad (\mathbf{x}, t) \in \partial D(t) \times [0, T], \tag{5}$$

or

$$\frac{\partial u}{\partial n}(\mathbf{x}, t) = h(\mathbf{x}, t), \quad (\mathbf{x}, t) \in \partial D(t) \times [0, T]. \tag{6}$$

Here Ω and $D(t)$ are simply connected bounded smooth domains such that $\overline{D(t)} \subset \Omega$ and $\Omega \setminus D(t)$ is connected, $T > 0$ is an arbitrary time of interest and $\mathbf{n}$ is the outward unit normal to the boundary. The functions $u_0(\mathbf{x}), f(\mathbf{x}, t), g(\mathbf{x}, t)$ and $h(\mathbf{x}, t)$ are known. The related inverse boundary determination problem which arises in corrosion engineering and in which ∂D consists of an unknown portion of $\partial\Omega$ has been investigated with the MFS in Hon and Li (2008). In (5) or (6) the function h is usually taken to be uniform, e.g. zero, such that $D(t)$ represents a rigid inclusion for the homogeneous Dirichlet boundary condition (5) and a cavity for the homogeneous Neumann boundary condition (6). Also the Neumann boundary condition (4) may be partially limited to a portion $\Sigma \times [T_0, T_1]$ of $\partial\Omega \times (0, T)$. The solution of the inverse problem (1)-(5), or (1)-(4), (6) is unique, see Chapko et al. (1998, 1999), respectively. However, the problems are still ill-posed since small errors in the input data (2)-(4) cause large deviations in the solution $(u(\mathbf{x}, t), D(t))$.

2. THE METHOD OF FUNDAMENTAL SOLUTIONS

The method of fundamental solutions (MFS) is a powerful meshless method which can be used to obtain accurate solutions to linear partial differential equations. The MFS assumes that the solution of the heat equation can be approximated by a linear combination of fundamental solutions of the form [5],

$$U_{M,N}(\mathbf{x}, t) = \sum_{m=1}^{2M} \sum_{j=1}^{2N} c_j^m F(\mathbf{x}, t; \mathbf{y}_j^m, \tau_m), \quad (\mathbf{x}, t) \in (\overline{\Omega} \setminus D(t)) \times [0, T], \tag{7}$$

where $(\mathbf{y}_j^m)_{j=\overline{1,2N}}^{m=\overline{1,2M}}$ are space 'singularities' located outside the space domain $\overline{\Omega} \setminus D(t)$, τ_m are times located in the interval $(-T, T)$ and F is the fundamental solution for the two-dimensional heat equation given by

$$F(\mathbf{x}, t; \mathbf{y}, \tau) = \frac{H(t - \tau)}{4\pi(t - \tau)} exp\left(-\frac{|\mathbf{x} - \mathbf{y}|^2}{4(t - \tau)}\right), \tag{8}$$

where H is the Heaviside function which is included in order to emphasize that the fundamental solution is zero for $t \leq \tau$.

Without loss of generality based on the conformal mapping theorem we can assume that the smooth, bounded and simply-connected domain Ω is the unit disk B(0,1). Furthermore, for simplicity, we assume that the smooth, simply-connected domain $\overline{D}(t) \subset \Omega$ is star-shaped with respect to the origin, hence its boundary, $\partial D(t)$ can be represented in parametric polar form by a 2π - periodic smooth function $r : [0, 2\pi) \times [0, T] \to (0, 1)$ as

$$\partial D(t) = \left\{ \big(r(\theta, t)cos(\theta), r(\theta, t)sin(\theta) \big) \mid \theta \in [0, 2\pi) \right\}, \quad t \in [0, T]. \tag{9}$$

In three-dimensions one can use spherical coordinates.

In the direct problem, when the domain $D(t)$ is known, the unknown coefficients $(c_j^m)_{j=\overline{1,2N}}^{m=\overline{1,2M}}$ in the MFS expansion (7) are determined by collocating the initial condition (2) and either of the

boundary conditions (3) or (4), and (5) or (6). In the inverse problem, the unknown coefficients $(c_j^m)_{j=\overline{1,2N}}^{m=\overline{1,2M}}$ and also some time-dependent radii $(\mathbf{r}_j^m)_{j=\overline{1,N}}^{m=\overline{0,M}}$ are to be determined by collocating equations (2)-(4) and (5) or (6)

1.1 DISTRIBUTION OF SOURCE AND COLLOCATION POINTS

In this section we describe how source and boundary collocation points are distributed for problems in which the outer boundary $\partial\Omega$ is a circle of radius 1 and the inner boundary $\partial D(t)$ is that of a star-shaped domain. The outer source points are located outside $\Omega = B(\mathbf{0}, 1)$ on a circle $\partial B(\mathbf{0}, R)$ of radius $R > 1$, namely

$$\mathbf{y}_j^m = (Rcos(\theta_j), Rsin(\theta_j)), \quad \theta_j = \frac{2\pi j}{N}, \quad j = \overline{1,N}, \quad m = \overline{1,2M} \tag{10}$$

We also take

$$\tau_m = \begin{cases} \frac{(2m-1)T}{2M}, & m = \overline{1,M} \\ \\ -\frac{[2(m-M)-1]T}{2M}, & m = \overline{M+1,2M} \end{cases} \tag{11}$$

The inner source points are located inside $D(t)$, namely,

$$\mathbf{y}_{j+N}^m = \frac{1}{2}(r_j^m cos(\theta_j), r_j^m sin(\theta_j)), \quad j = \overline{1,N}, \quad m = \overline{1,2M} \tag{12}$$

where the radii $r(\theta_j, \tau_m) = r_j^m \in (0,1)$ constitute a radial parameterisation of the star shaped domain $D(t)$ whose boundary at time t is approximated by, see (9),

$$\partial D(t) = \left\{ (r(\theta_j, t)cos(\theta_j), r(\theta_j, t)sin(\theta_j)) \mid j = \overline{1,N} \right\}, \quad t \in (-T, T), \tag{13}$$

and we have taken symmetric $\partial D(-t) = \partial D(t)$ for $t \in (0, T)$. From (10) and (12) one can see that a total of $4MN$ source points have been specified. We now specify the collocation points.

On the outer boundary we take boundary $\partial\Omega$ we take the boundary collocation points

$$(\mathbf{x}_i, \tau_j) = (cos(\theta_i), sin(\theta_i), \tau_j), \quad i = \overline{1,N}, \quad j = \overline{0,M}, \tag{14}$$

where $\tau_0 = 0$.
On the inner boundary $\partial D(t)$ we take the boundary collocation points

$$(\mathbf{x}_i^j, \tau_j) = (r_i^j cos(\theta_i), r_i^j sin(\theta_i), \tau_j), \quad i = \overline{1,N}, \quad j = \overline{0,M}. \tag{15}$$

Collocating the boundary conditions (3)-(5) results in $3(M+1)N$ equations. Another $(K-1)N$ equations are obtained by imposing the initial condition (2). We collocate the initial condition (2) in the domain $\Omega \setminus \overline{D(0)}$ at time $t = 0$ at the points

$$\mathbf{x}_{i,j} = \left(\left(r_j^0 + \frac{(1-r_j^0)i}{K} \right)cos(\theta_j), \left(r_j^0 + \frac{(1-r_j^0)i}{K} \right)sin(\theta_j) \right), \quad i = \overline{1,(K-1)}, \quad j = \overline{1,N}, \tag{16}$$

where $r_j^0 = r(\theta_j, 0)$ for $j = \overline{1,N}$.
    The final problem entails $4MN + N(M+1) = N(5M+1)$ unknowns represented by the $4MN$ coeffcents $\mathbf{c} = (c_j^m)_{j=\overline{1,2N}}^{m=\overline{1,2M}}$ in the MFS expression (7), and the $N(M+1)$ radii $\mathbf{r} = (r_j^m)_{j=\overline{1,N}}^{m=\overline{0,M}}$. On the other hand the collocation of the conditions (2)-(5) amounts to $N(3M + K + 2)$ equations, namely, $(K-1)N$ equations for the initial condition (2) imposed at the points (15),

$2(M + 1)N$ equations for the Cauchy boundary condition (3) and (4) imposed at the points (14), and $(M + 1)N$ equations for the boundary condition (5) or (6) imposed at the points (13). From the above counting it follows that a necessary solution for a unique solution is $K \geq 2M - 1$.

1.2 LEAST-SQUARES MINIMISATION

As the boundary conditions (3)-(5) and initial condition (2) are known we can fit the approximated data of the MFS to these values using a nonlinear least-squares formulation to find the unknown values of $\mathbf{c}$ and $\mathbf{r}$, namely, we minimise the functional

$$S(\mathbf{c}, \mathbf{r}) = ||U_{M,N} - f||^2 + ||U_{M,N} - h||^2 + \left|\left|\frac{\partial U_{M,N}}{\partial n} - g\right|\right|^2 + ||U_{M,N} - u_0||^2. \qquad (17)$$

In discretised form, expression (17) to be minimized can be written as:

$$S(\mathbf{c}, \mathbf{r}) = \sum_{i=1}^{N} \sum_{j=0}^{M} \left[(U_{M,N}(\mathbf{x}_i, \tau_j) - f(\mathbf{x}_i, \tau_j))^2 + \left(\frac{\partial U_{M,N}}{\partial n}(\mathbf{x}_i, \tau_j) - g(\mathbf{x}_i, \tau_j)\right)^2 \right]$$

$$+ \sum_{i=1}^{N} \sum_{j=1}^{M} \left(U_{M,N}(\mathbf{x}_i^j, \tau_j) - h(\mathbf{x}_i^j, \tau_j) \right)^2 + \sum_{i=1}^{K-1} \sum_{l=1}^{N} (U_{M,N}(\mathbf{x}_{i,l}, 0) - u_0(\mathbf{x}_{i,l}))^2. \qquad (18)$$

In expressing the second term in (17) the normal derivative of the fundamental solution (7) is needed, namely

$$\frac{\partial F}{\partial n}(\mathbf{x}, t; \mathbf{y}, \tau) = -\frac{(\mathbf{x} - \mathbf{y}) \cdot \mathbf{n}}{8\pi(t - \tau)^2} \, exp\left(-\frac{|\mathbf{x} - \mathbf{y}|^2}{4(t - \tau)} \right) H(t - \tau). \qquad (19)$$

The minimisation of (18) is performed using the optimisation toolbox function 'fmincon' in MATLAB. The 'fmincon' toolbox employs an 'interior point' algorithm [2]. In our work this algorithm minimizes (18) subject to the constraints $\mathbf{0} < \mathbf{r} < \mathbf{1}$ that the defect $\overline{D(t)}$ stays within the fixed host domain Ω during the iterations.

As parallel computers become more and more powerful, more attention is being paid recently to solve inverse problems on supercomputers. Inverse problems are much more difficult and expensive to solve than forward problems. Due to the large number of unknowns the minimization program is highly computationally intensive. In order to carry out the computations in a reasonable time frame, a parallel computing approach is implemented. In order to achieve this, the MATLAB toolbox is used and the code is run on the University of Leeds 'ARC1' high performance computer. The MATLAB function 'fmincon' has inbuilt parallel functionality. When using either the linear, Newtonian step or conjugate gradient step the gradient of both the objective and constraint functions are required. The MATLAB optimisation toolbox calculates this gradient using finite differencing about points close to the current point $\mathbf{x}$. The parallel toolbox allows this finite differencing process to occur in parallel and thus speed up the minimisation process. In order to demonstrate the benefits of using such a tool, computational timings for various total number of points, $N(5M + 1)$ when $K = 2M - 1$, have been provided below.
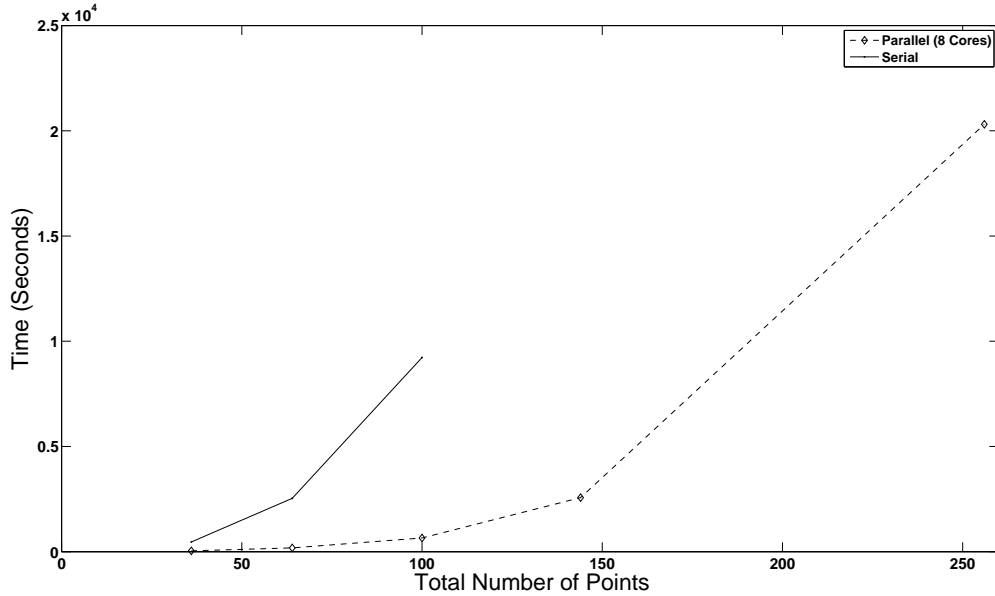
Figure 1: Comparison of computational times for runs in parallel and serial.

3. NUMERICAL RESULTS AND DISCUSSION

As an illustrative simple example, in this section we attempt to locate a stationary star-shaped inclusion $D(t)$ $B(\mathbf{0}, 0.5)$ within the domain $\Omega = B(\mathbf{0}, 1)$.

The initial and boundary conditions (2), (3) and (5) are given by

$$u(\mathbf{x}, 0) = u_0(\mathbf{x}) = |\mathbf{x}|^2, \quad \mathbf{x} \in \overline{\Omega} \setminus D(0), \tag{20}$$

$$u(\mathbf{x}, t) = f(\mathbf{x}, t) = 4t + 1, \quad (\mathbf{x}, t) \in \partial\Omega \times [0, T], \tag{21}$$

$$u(\mathbf{x}, t) = h(\mathbf{x}, t) = 4t + 0.25, \quad (\mathbf{x}, t) \in \partial D(t) \times [0, T]. \tag{22}$$

As described previously, the inverse problem here is a difficult non-linear ill-posed problem and therefore extra information is needed in order to reconstruct the moving boundary, $\partial D(t)$, within the domain Ω. This information is in the form of the heat flux on $\partial\Omega$, as described by equation (4), namely

$$\frac{\partial u}{\partial n}(x, t) = g(\mathbf{x}, t) = 2, \quad (\mathbf{x}, t) \in \partial\Omega \times [0, T]. \tag{23}$$

The initial guess was taken as $\mathbf{r} = \mathbf{0.8}$ and $\mathbf{c} = \mathbf{0.1}$. The accuracy of the solution was analysed using the R.M.S value of the error between the analytical and estimated internal boundary defined as,

$$\text{RMS} = \sqrt{\frac{\sum_{j=1}^{N} \sum_{m=0}^{M} \left(r_j^m - 0.5 \right)^2}{N(M+1)}}. \tag{24}$$

As such, if the boundary is located exactly the R.M.S value would be zero.

The program was run for a variety of MFS parameters, although a parameter set of $M = N = 12$, $K = 23$ was deemed sufficiently large for the purposes of achieving an accurate result when balanced with the high computational time required for larger MFS parameter values. It can be clearly seen from the results presented in Table 1 that as the parameter size increases, the overall accuracy of the estimated solution increases.

181

Size	Obj. Func.	RMS	CPU Time (s)	Iterations
$M = N = 6,\ K = 11$	1.00612	0.145203	16.587	61
$M = N = 8,\ K = 15$	0.08784	0.03370	72.736	68
$M = N = 10,\ K = 19$	0.04311	0.01897	336.55	105
$M = N = 12,\ K = 23$	0.02623	0.00931	1116.8	113

Table 1: Numerical results for the objective function (18), the RMS (27), the CPU time and the number of iterations required for convergence, obtained with various MFS parameter sizes.

In reality, the heat flux values (4) on the boundary $\partial\Omega$ would be measured using experimental techniques. Due to this, a numerical noise factor is numerically simulated to mimic the inherent errors in the experimental data that would be used. Noisy data was achieved by using the MATLAB function $normrand(0, \sigma)$, which generates a random number from a given normal distribution space, namely,

$$g^{\eta}(\mathbf{x}_i^j, t_j) = g(\mathbf{x}_i^j, t_j) + \epsilon_{i,j} = 2 + \epsilon_{i,j}, \quad i = \overline{1, N}, \quad j = \overline{0, M}, \tag{25}$$

where $\epsilon_{i,j}$ are normal random variables with mean 0 and standard deviation $\sigma = 2p\%$, where p represents the percentage of noise.

Figures 7 and 8 show the corresponding objective function (18) being minimized and the RMS value (27), as functions of the number of iterations, respectively, for $p = 10\%$ noise added in the flux data (26), as in (28).
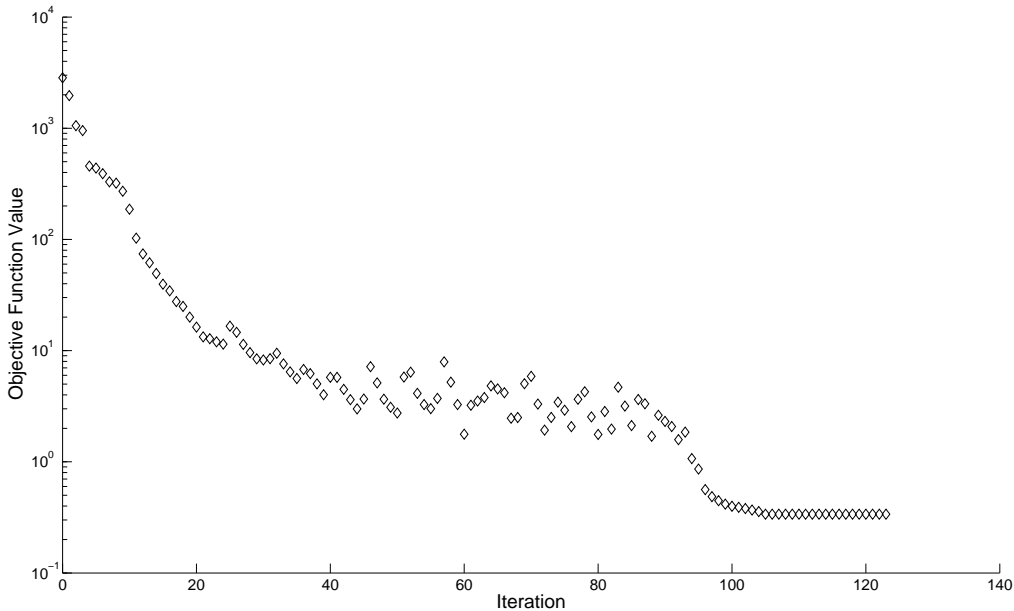

Figure 2: Plot of the objective function for MFS parameters $M = N = 12, K = 23$, for $p = 10\%$ noise. After 107 iterations the function (18) reached a value of 0.33766.
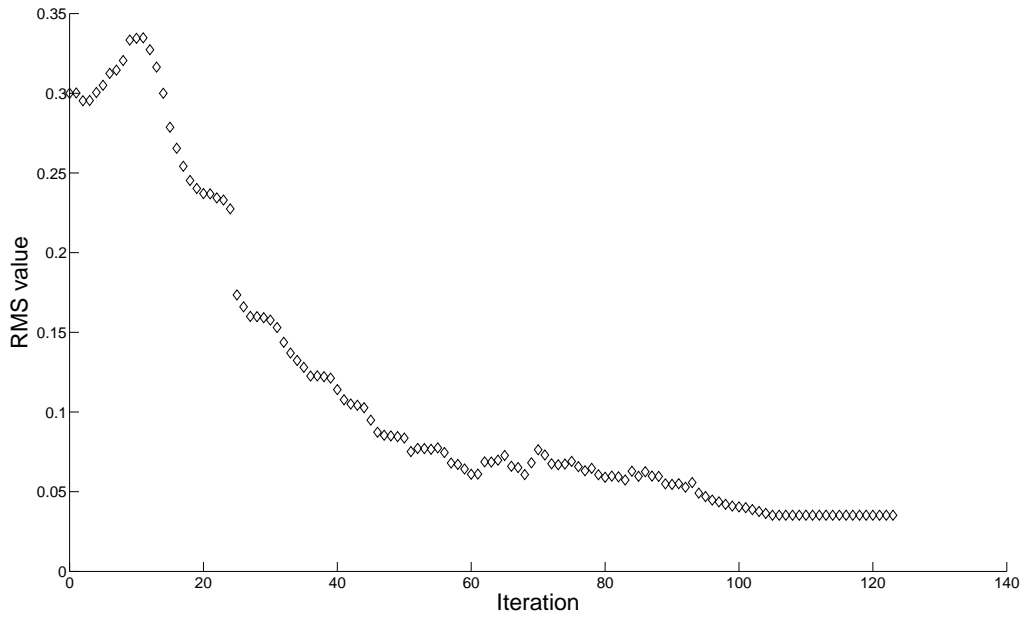
Figure 3: Plot of RMS value for MFS parameters $M = N = 12, K = 23$, for $p = 10\%$ noise. After 107 iterations the function (27) reached a value of 0.03523.

From these figures it can be seen that introducing noise decreases the accuracy and stability of the solution, however to make this clearer, a graphical representation of the solution is given in Figure 9.
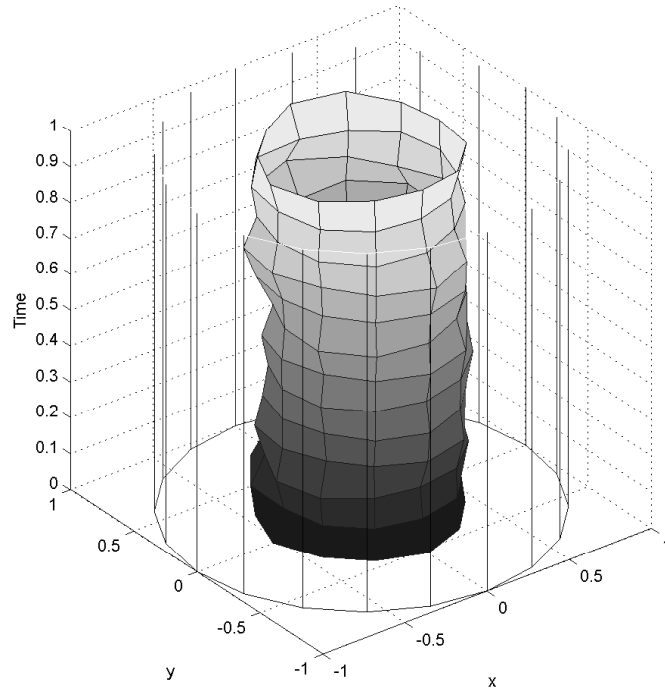

Figure 4: Final plot of the inclusion after the final 107 iterations. $M = N = 12$, $K = 23$, $p = 10\%$ noise.

From Table 2 it can be seen that as the amount of noise decreases the numerical solution approximates better the exact solution.

Overall, the numerical results obtained for Example 1 demonstrate that the MFS provides a powerful method for solving inverse geometric problems concerned with the reconstruction of simple smooth internal boundaries, such as a circle. The method provides a simpler alternative from using methods such as the boundary element method (BEM) or the finite element method (FEM), which can often be complicated when meshing moving geometries. It was shown that high levels of accuracy and resolution can be obtained for a simple geometry such as a circular inclusion, however, the addition of noise in the input data can cause a decrease in the resolution and stability.

Noise (%)	Obj. Func.	RMS	Iterations
0	0.02623	0.00931	112
5	0.10689	0.02030	109
10	0.33766	0.03523	107
25	2.57784	0.10168	111

Table 2: Numerical results for the objective function (18), the RMS (27) and the number of iterations required for convergence, obtained with $M = N = 12$, $K = 23$ and various levels of noise.

REFERENCES

1. D. Borman, D.B. Ingham, B. T. Johansson and D. Lesnic (2009) The method of fundamental solutions for detection of cavities in EIT, *Journal of Intergral Equations and Applications*, **21**, 383-406.

2. R.H. Byrd, J.C. Gilbert, and J. Nocedal (2000) A trust region method based on interior point techniques for nonlinear programming, *Mathematical Programming*, **89**, 149-185

3. R. Chapko, R. Kress and J.-R. Yoon (1998) On the numerical solution of an inverse boundary value problem for the heat equation, *Inverse Problems*, **14**, 853-867.

4. R. Chapko, R. Kress and J.-R. Yoon (1999) An inverse boundary value problem for the heat equation: the Neumann condition, *Inverse Problems*, **15**, 1033-1046.

5. A. Karageorghis and D. Lesnic (2009) Detection of cavities using the method of fundamental solutions, *Inverse Problems in Science and Engineering*, **17**, 803-820.

6. A. Karageorghis, and D. Lesnic (2011) Application of the MFS to inverse scattering problems, *Engineering Analysis with Boundary Elements*, **35**, 631-638.

7. B.T. Johansson, D. Lesnic and T. Reeve A method of fundamental solutions for two-dimensional heat conduction, *International Journal of Computer Mathematics* (in press).

8. Y.C. Hon and M. Li (2008) A computational method for inverse free boundary determination problem, *International Journal for Numerical Methods in Engineering*, **73**, 1291-1309.